Check for updates

Application of response surface methodology as a new PID tuning method in an electrocoagulation process control case

Ş. Camcıoğlu, B. Özyurt, İ. C. Doğan and H. Hapoğlu

ABSTRACT

In this work the application of response surface methodology (RSM) to proportional-integral-derivative (PID) controller parameter tuning for electrocoagulation (EC) treatment of pulp and paper mill wastewater was researched. Dynamic data for two controlled variables (pH and electrical conductivity) were obtained under pseudo random binary sequence (PRBS) input signals applied to manipulated variables (acid and supporting electrolyte flow rates). Third order plus time delay model parameters were evaluated through System Identification Toolbox™ in MATLAB®. Four level full factorial design was applied to form a design matrix for three controller tuning parameters as factors and to evaluate statistical analysis of the system in terms of integral of square error (ISE), integral of absolute error (IAE), integral of time square error (ITSE) and integral of time absolute error (ITAE) performance criteria as response. Numerical values of the responses for the runs in the design matrices were determined using closed-loop PID control system simulations designed in Simulink®. Optimum proportional gain, integral action and derivative action values for electrical conductivity control were found to be 1,500 s, 0 s and 16.4636 s respectively. Accordingly, the same optimization scheme was followed for pH control and optimum controller parameters were found to be −8.6970 s, 0.0211 s and 50 s, respectively. Theoretically optimized controller parameters were applied to batch experimental studies. Chemical oxygen demand (COD) removal efficiency and energy consumption of pulp and paper mill wastewater treatment by EC under controlled action of pH at 5.5 and electrical conductivity at 2.72 mS/cm was found to be 85% and 3.87 kWh/m^3 respectively. Results showed that multi input–multi output (MIMO) control action increased removal efficiency of COD by 15.41% and reduced energy consumption by 6.52% in comparison with treatment under uncontrolled conditions.

Key words | electrochemical wastewater treatment, MIMO control, PID control, pulp and paper mill wastewater, response surface methodology

Ş. Camcıoğlu (corresponding author)
B. Özyurt
İ. C. Doğan
H. Hapoğlu
Ankara University Faculty of Engineering
Department of Chemical Engineering,
Tandoğan, Ankara,
Turkey
E-mail: *camcioglu@eng.ankara.edu.tr*

INTRODUCTION

The pulp and paper industry has high pollutant discharges to the environment. Pulp and paper wastewater contains chlorinated compounds, phenols, lignin and sulphur compounds that are responsible for high total organic carbon (TOC), chemical oxygen demand (COD), colour and turbidity (Shankar *et al.* 2014). Discharge of these wastewaters into the environment without treatment increases the quantity of toxic substances in the receiving water and damages scenic beauty (Behrooz *et al.* 2011). It is reported that the most commonly used treatment methods of pulp and paper effluent are physical adsorption (Shawwa *et al.* 2001), chemical oxidation (Hassan & Hawkyard 2002), wet oxidation (Verenich *et al.* 2000) and biochemical methods (Rajeshwari *et al.* 2000; Raj *et al.* 2007). Biological treatment methods are not effective in pulp and paper wastewater treatment because of the low biodegradability of the wastewater (Aghdam *et al.* 2016). Besides, high sludge generation is the major disadvantage of chemical treatment (Camcıoğlu *et al.* 2016). Therefore, there has been an increasing interest in electrochemical methods for the treatment of pulp and paper effluent. Electrocoagulation (EC) is one of the alternative methods in wastewater treatment, resulting in the

doi: 10.2166/wst.2017.506

Downloaded from http://iwaponline.com/wst/article-pdf/76/12/3410/241768/wst076123410.pdf
by guest

coagulation of small charged colloidal particles. (Verenich *et al.* 2000; Raj *et al.* 2007). In recent years, EC has been reported as a simple, efficient and economical method and able to successfully treat different effluents, such as boron-containing wastewater (Xu *et al.* 2009), municipal wastewater (Moreno *et al.* 2013), textile wastewater (Mahmoodi & Dalvand 2013), dairy wastewater (Benaissa *et al.* 2016), industrial area wastewater (Yadav *et al.* 2012), tannery wastewater (Varank *et al.* 2016), water containing heavy metals (Vasudevan *et al.* 2012) and pulp and paper mill wastewater (Pokhrel & Viraraghavan 2004; Sridhar *et al.* 2011; Camcioglu *et al.* 2014; Asaithambi 2016).

Pulp and paper mill wastewater treatment by EC is a very complex process and is greatly influenced by many factors, including electrode configuration and material, current density, electrolysis time, pH, temperature and electrical conductivity (El-Ashtoukhy *et al.* 2009; Zaied & Bellakhal 2009; Sridhar *et al.* 2011). Temperature affects the efficiency of pollutant removal through reaction rates, fluid conductivity, metal hydroxide solubility and bubble generation (Phalakornkule *et al.* 2010). It is reported that aluminium solubility can be improved by increasing the solution temperature (Perry *et al.* 1984). The electrical conductivity of a solution depends on the ion concentration and the temperature (McCleskey *et al.* 2012). Control of electrical conductivity is crucial due to Ohm's law of resistance, as high values of electrical conductivity reduce the resistance, the potential difference and the power consumption of the EC process under constant current conditions (Terrazas *et al.* 2010). Chemical dissolution of metal electrodes is closely related to the pH value of the solution. In a certain pH range, the metal ions in the solution can form many coagulated species and metal hydroxides that adsorb dissolved contaminants and destabilize suspended particles (Cañizares *et al.* 2005; Merzouk *et al.* 2009). At low pH (2–3) the cationic monomeric species Al^{3+} and $Al(OH)^{+2}$ dominate. When pH is between 4 and 9, the Al^{3+} and OH^{-} ions generated by the electrodes react to form various monomeric species such as $Al(OH)_2^+$, $Al(OH)_2^{2+}$, and polymeric species such as $Al_6(OH)_{15}^{3+}$, $Al_7(OH)_{17}^{4+}$, $Al_{13}(OH)_{34}^{5+}$ that finally transform into insoluble amorphous $Al(OH)_{3(s)}$ through complex precipitation kinetics (Bayramoglu *et al.* 2004). When the pH is higher than 10, the monomeric $Al(OH)_4^-$ anion concentration increases (Alinsafi *et al.* 2005). It is reported that pH increases during the EC process (Demirci *et al.* 2015). Accordingly, the formation of ionic compounds that have high solubility in water cause a decrease in removal efficiencies. As a result, the control of temperature, pH and electrical conductivity at their optimum values is essential.

Proportional-integral-derivative (PID) control provides the simplest and most effective solution to many real-world control problems by means of three-term functionality covering treatment to both transient and steady state responses (Ang *et al.* 2005). Various studies were reported for tuning PID controllers in the literature with monotonic transient responses (Ziegler & Nichols 1942; Cohen & Coon 1953; Hang *et al.* 1991; Astrom *et al.* 1993; Abbas 1997; Wang *et al.* 1999). Designing and tuning a PID controller appears to be conceptually intuitive, but can be practically difficult if multiple (and often conflicting) goals such as short transient response time and high stability are to be reached (Cominos & Munro 2002; Altinten *et al.* 2004). Generally, the initial designs should be repeatedly adjusted by computer simulations until a desirable closed-loop system performance is achieved (Ang *et al.* 2005). There are many factors that influence the effect of PID control, and among the most important is selection of the three parameters proportional gain, integral time constant and derivative time constant (Liu *et al.* 2017). Parameter selection is a combinatorial optimization problem and the result directly determines the effect of PID control; thus, parameter tuning plays an important role in evaluating the performance of a PID controller (Liu *et al.* 2017). The velocity form of the digital PID controller is given in Equation (1), where the values of the controller output at each sampling time are calculated (Karacan *et al.* 1997).

$$u(t) = u(t-1) + K_c\left[(\varepsilon(t) - \varepsilon(t-1)) + \frac{\Delta t}{\tau_I}\varepsilon(t) + \frac{\tau_D}{\Delta t}(\varepsilon(t) - 2\varepsilon(t-1) + \varepsilon(t-2))\right] \quad (1)$$

Here, u(t) is the controller output, K_C is the proportional gain, τ_I is the integral time constant, τ_D is the derivative time constant, Δt is the sample time and $\varepsilon(t)$ is the error that is the difference between a set point and a measured value of the controlled variable. According to the equation above, when the measured value exceeds the set point, $\varepsilon(t)$ will be negative, so that the controller output will decrease. In some cases, such as control of rising pH using acidic solutions, process dynamics require an inverted controller action. Such an action can be obtained with a negative K_C selection.

The objectives of this study were to apply response surface methodology (RSM) as a new tuning strategy to optimize PID controller performances for pH and electrical conductivity parameters of an EC process in which pulp and paper mill wastewater was treated, and to determine the effects of control action on pollutant removal and energy consumption values.

Downloaded from http://iwaponline.com/wst/article-pdf/76/12/3410/241768/wst076123410.pdf
by guest

Theoretically optimized PID parameters for pH and electrical conductivity controllers were applied to batch experimental studies to evaluate the performances of the controllers. COD, colour, turbidity, total suspended solids (TSS) removal efficiencies and energy consumption values were compared with uncontrolled treatment results.

METHODS

Real wastewater obtained from a pulp and paper mill in Turkey was used in this study. Table 1 shows the characteristics of the wastewater.

In this study, pH and electrical conductivity were selected as controlled variables; acid and supporting electrolyte flow rates were selected as manipulated variables. Pseudo random binary sequence (PRBS) input signals were applied to the manipulated variables for dynamic analyses of pH and electrical conductivity. Obtained dynamic data were used to evaluate third order plus time delay (TOPTD) models' parameters using System Identification Toolbox™ in MATLAB®.

For each controller, four level full factorial design was applied to form a design matrix using K_C, τ_I and τ_D parameters as factors. The levels of factors and design matrices for pH and electrical conductivity are given in Tables 2 and 3 respectively. Integral of square error (ISE), integral of absolute error (IAE), integral of time square error (ITSE) and integral of time absolute error (ITAE) performance criteria which are given below in Equations (2)–(5) were calculated for each run as response. Since performance criteria depends on the error, the lower values of ISE, IAE, ITAE and ITSE are indicators of better performance (Altuntaş & Hapoğlu 2016).

$$ISE = \int_0^\infty \varepsilon^2(t)\,dt \tag{2}$$

Table 1 | Characteristics of pulp and paper mill wastewater

Parameter	Unit	Value
pH	–	6.45
Electrical conductivity	mS/cm	2.60
COD	mg/L	386.772
Colour	CU	1,441.152
Turbidity	NTU	104.25
TSS	mg/L	54.64

Table 2 | The levels of PID parameters

	Factors			Factors		
	Electrical conductivity			pH		
Level	K_C	τ_I	τ_D	K_C	τ_I	τ_D
−2	750	0.00005	0.1	−9	0.008	25
−1	1,000	0.000125	7.6	−7	0.016	50
+1	1,250	0.000175	15.1	−5	0.024	75
+2	1,500	0.000225	22.6	−3	0.032	100

$$IAE = \int_0^\infty |\varepsilon(t)|\,dt \tag{3}$$

$$ITAE = \int_0^\infty t.\ |\varepsilon(t)|dt \tag{4}$$

$$ITSE = \int_0^\infty t.\varepsilon^2(t)dt \tag{5}$$

Design matrices were implemented using PID control system simulations shown in Figure 1, which were designed in Simulink® using TOPTD models of pH and electrical conductivity parameters. According to the results obtained, PID parameters for pH and conductivity were optimized theoretically for each controller in MINITAB 17 software. Theoretical control application for pH and conductivity were performed with these PID parameters by using closed-loop PID control system simulations. Controller performances are compared with three different tuning methods: Cohen–Coon (Cohen & Coon 1953), Ziegler–Nichols (Ziegler & Nichols 1942) and Control System Toolbox™ (CST) in MATLAB®. PID parameters were then applied to batch experimental studies of pH and electrical conductivity control under constant temperature to determine removal efficiencies and energy consumption. EC treatment of pulp and paper mill wastewater without control action was also performed to compare the results.

Energy consumption values were calculated per cubic metre of wastewater treated using the logged voltage–time data considering Equation (6) given below.

$$\text{Energy consumption (kWh/m}^3) = \frac{I V_m t}{V_E} \tag{6}$$

Downloaded from http://iwaponline.com/wst/article-pdf/76/12/3410/241768/wst076123410.pdf
by guest

Table 3 | Design matrices of electrical conductivity and pH processes

	Electrical conductivity			pH		
Run	K_C	τ_I	τ_D	K_C	τ_I	τ_D
1	750	0.000125	7.6	−3	0.024	50
2	1,500	0.000225	0.1	−3	0.024	25
3	1,000	0.000125	15.1	−5	0.016	100
4	750	0.000175	15.1	−7	0.008	25
5	1,250	0.00005	22.6	−9	0.032	100
6	750	0.000225	7.6	−9	0.008	75
7	1,000	0.00005	15.1	−7	0.032	25
8	1,500	0.000175	0.1	−9	0.032	50
9	1,000	0.000125	0.1	−7	0.032	50
10	1,500	0.000125	7.6	−3	0.008	25
11	1,000	0.000175	22.6	−3	0.032	100
12	1,250	0.000225	7.6	−3	0.032	75
13	1,250	0.00005	15.1	−7	0.016	25
14	1,500	0.00005	22.6	−3	0.008	100
15	1,500	0.000175	15.1	−9	0.024	100
16	750	0.000225	0.1	−9	0.024	50
17	750	0.000125	15.1	−7	0.024	25
18	1,250	0.000125	22.6	−5	0.016	50
19	1,500	0.000125	22.6	−3	0.032	25
20	1,250	0.000175	0.1	−5	0.008	25
21	1,250	0.000225	0.1	−3	0.016	25
22	750	0.00005	22.6	−7	0.032	100
23	1,000	0.000175	15.1	−3	0.024	100
24	750	0.000125	22.6	−9	0.016	25
25	750	0.000225	15.1	−9	0.008	25
26	1,250	0.000225	22.6	−7	0.016	100
27	750	0.000225	22.6	−3	0.032	50
28	1,000	0.000125	7.6	−5	0.032	25
29	750	0.000175	7.6	−7	0.024	50
30	1,250	0.000125	0.1	−7	0.024	75
31	1,500	0.000125	15.1	−3	0.008	50
32	1,000	0.000225	22.6	−3	0.016	100
33	750	0.00005	15.1	−9	0.008	50
34	1,500	0.000125	0.1	−9	0.032	25
35	1,500	0.00005	0.1	−7	0.008	50
36	750	0.00005	0.1	−9	0.024	25
37	1,500	0.000175	7.6	−9	0.032	75
38	1,250	0.000125	15.1	−5	0.024	50
39	1,500	0.000175	22.6	−5	0.032	50
40	1,000	0.000125	22.6	−3	0.008	75
41	750	0.00005	7.6	−9	0.016	75
42	1,000	0.000225	7.6	−5	0.008	50
43	750	0.000175	0.1	−9	0.024	75
44	1,000	0.00005	7.6	−7	0.016	75
45	1,500	0.00005	7.6	−7	0.032	75
46	1,250	0.000175	15.1	−5	0.008	100
47	750	0.000175	22.6	−9	0.016	100
48	1,500	0.000225	7.6	−9	0.008	100
49	1,000	0.000175	7.6	−5	0.016	25
50	1,250	0.00005	0.1	−9	0.016	50
51	1,250	0.000125	7.6	−5	0.032	75
52	1,250	0.000175	22.6	−7	0.008	75
53	1,000	0.000225	0.1	−5	0.032	100
54	1,250	0.000225	15.1	−7	0.008	100
55	750	0.000125	0.1	−5	0.024	25
56	1,000	0.000225	15.1	−3	0.024	75
57	1,000	0.000175	0.1	−3	0.016	75
58	1,500	0.00005	15.1	−7	0.016	50
59	1,000	0.00005	0.1	−5	0.008	75
60	1,250	0.00005	7.6	−5	0.024	75
61	1,500	0.000225	22.6	−5	0.024	100
62	1,000	0.00005	22.6	−7	0.024	100
63	1,250	0.000175	7.6	−5	0.016	75
64	1,500	0.000225	15.1	−3	0.016	50

I is the applied current intensity in A, V_m is the mean potential difference applied in V, t is the duration of treatment in hours and V_E is the volume of treated wastewater in L. All removal efficiency and energy consumption calculations were made on the basis of sedimented wastewater characteristics (Table 1).

Experimental studies were carried out in a 2 L plexiglas reactor with six aluminium electrodes placed in a monopolar parallel arrangement. 1 L of wastewater was fed to the reactor before each experiment. Cooling water from a refrigerated circulating bath (Hoefer RCB20-PLUS) at 12.5 °C was passed through the jacket around the reactor by means of an on–off valve to keep the reaction temperature constant at 15 °C. The changes in electrical conductivity, pH and temperature of the wastewater were monitored and measured online by sensors (Mettler

Downloaded from http://iwaponline.com/wst/article-pdf/76/12/3410/241768/wst076123410.pdf
by guest

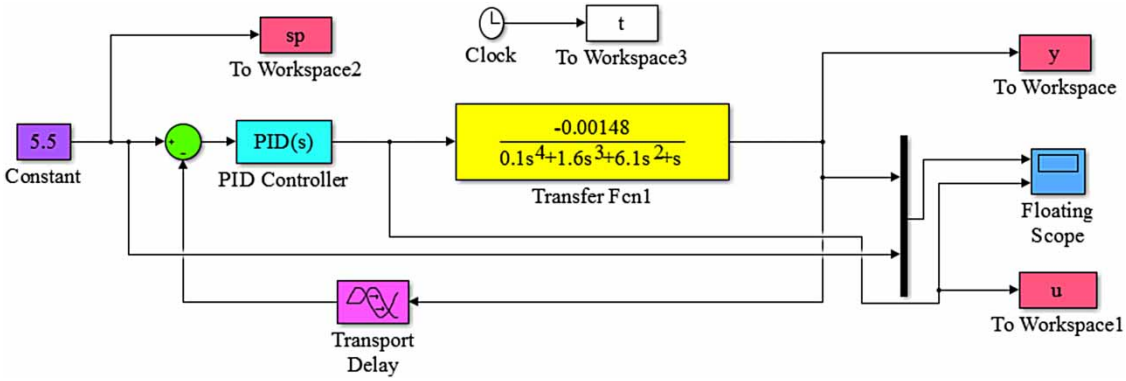

Figure 1 | Closed-loop PID control system simulation.

Toledo M200 Easy) during the experiments. A constant current DC power supply (MAY 11-PS Constant Current Power Supply) was used to maintain current intensity constant at a value of 1.22 A. A stirrer (MTOPS MS3200) was operated at 600 rpm in order to eliminate mass transfer resistances. Dynamic analyses and control studies were performed with 0.5 M HCl and 0.04 M NaCl as acid and supporting electrolyte solutions, respectively. The experimental set-up is shown in Figure 2.

10 ml samples were taken at 5 min intervals during the experiments to determine COD removal. At the end of 15 min of operations 250 ml samples were taken to analyse COD, colour, turbidity and TSS values. Analyses were carried out according to SM 5220 D, 2120 C, 2130 B and 2540 D respectively (APHA/AWWA/WEF 2005). 1.5 ml high range digestion solution and 3.5 ml sulfuric acid reagent were added to 2.5 ml samples in 16×100 mm culture tubes. Digestion of treated samples was carried out at 150 °C for 2 hours using a thermo-reactor (Velp ECO-16). Absorbance of Cr^{3+} ions in the digested samples was read at 600 nm using a spectrophotometer (PG Instruments T60 V). A calibration curve prepared using potassium

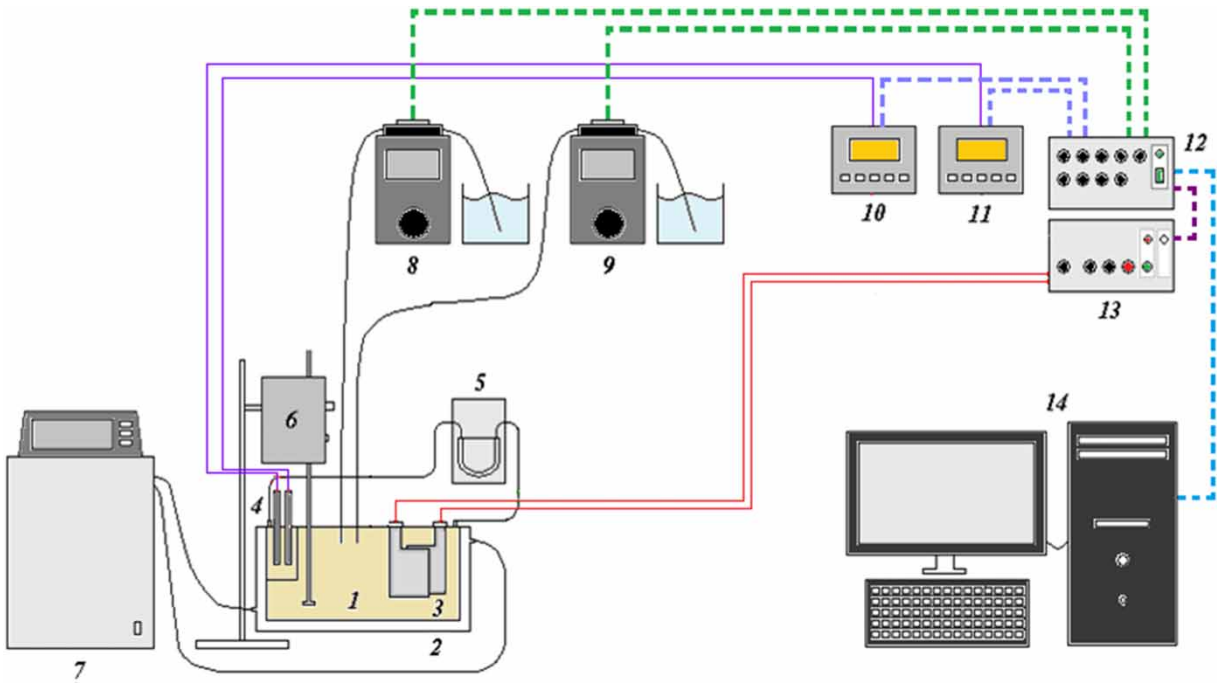

Figure 2 | Experimental set-up. 1: EC reactor, 2: heating/cooling jacket, 3: electrodes, 4: pH meter, electrical conductivity meter, thermocouple, 5: sample circulation pump, 6: mechanical stirrer, 7: refrigerated circulating bath, 8: acid solution pump, 9: supporting electrolyte solution pump, 10: pH and temperature display, 11: electrical conductivity display, 12: control unit, 13: power supply, 14: computer.

Downloaded from http://iwaponline.com/wst/article-pdf/76/12/3410/241768/wst076123410.pdf
by guest

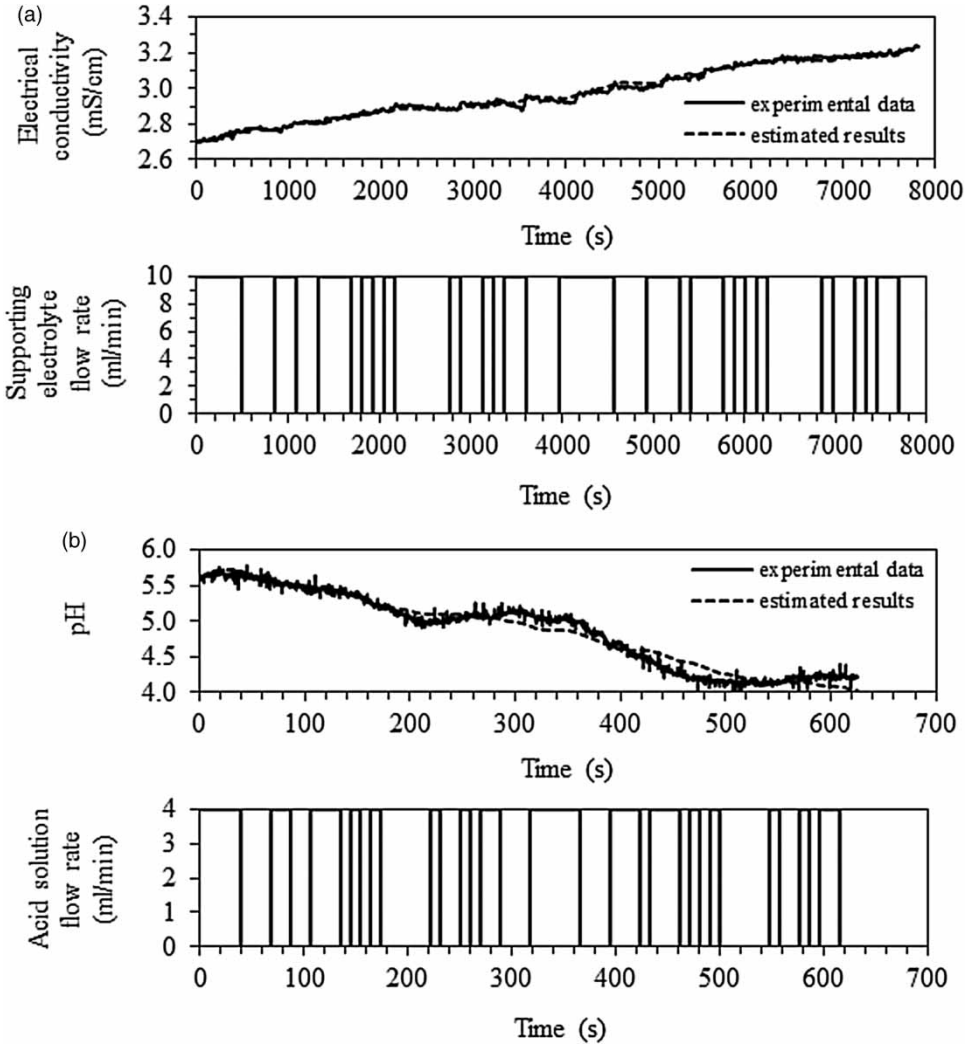

Figure 3 | Dynamic analyses and system identification results of (a) electrical conductivity and (b) pH processes under PRBS signal.

hydrogen phthalate standards was used to calculate the COD values of the samples. Colour determination of the samples in quartz cuvettes with 1 cm path length were performed at 456 nm using the spectrophotometer. A calibration curve prepared using 500 CU Pt–Co stock solution was used to calculate the colour values of the samples. Sample turbidity was measured using a turbidity meter (Aqualytic AL250T-IR). TSS analyses were performed using a Büchner flask and funnel, a vacuum pump (Rocker 410) and 1.2 μm pore diameter glass fibre filter paper. After filtration, the filter paper was dried at 105 °C in an oven (Memmert UN 55) at least 1 hour and weighed on an analytical balance (Bel Engineering M214Ai). This cycle of drying and weighing was repeated until a constant weight was obtained.

RESULTS AND DISCUSSION

PRBS signals were used to disturb the systems which were initially at steady state and to determine the dynamics of electrical conductivity and pH parameters. Figure 3 presents the variation of controlled and manipulated variables with time under PRBS signals. Experimental results were fitted to TOPTD models via System Identification Toolbox™ in MATLAB®. Model parameters of electrical conductivity and pH processes were estimated using the data obtained from dynamic analyses. Estimated results from system identification are also given in Figure 3 and transfer functions for electrical conductivity and pH processes are presented in Equations (7) and (8). High determination coefficients (R^2) of 90.63 and 80.28 for electrical conductivity and pH respectively

Downloaded from http://iwaponline.com/wst/article-pdf/76/12/3410/241768/wst076123410.pdf
by guest

Table 4 | Simulation results of four level full factorial design matrices for electrical conductivity and pH processes

	Electrical conductivity				pH			
Run	ISE	IAE	ITAE	ITSE	ISE	IAE	ITAE	ITSE
1	1,437,459	1,486,734	6×10^{8}	52,057,067	26,909	10,713	26,781,735	6.72714×10^{7}
2	928,369	1,080,325	4.58×10^{8}	26,286,576	42,985	14,995	37,486,312	1.07464×10^{8}
3	666,390	965,956	4.37×10^{8}	20,697,335	6,248	2,678	6,695,659	1.56205×10^{7}
4	1,207,569	1,589,660	7.76×10^{8}	59,210,655	5,568	2,308	5,769,588	1.39190×10^{7}
5	266,967	515,062	1.59×10^{8}	7,463,578	23,905	7,503	18,756,829	5.97635×10^{7}
6	1,444,389	1,727,284	9.14×10^{8}	70,177,363	3,600	1,633	4,083,133	9.00064×10^{6}
7	665,782	798,657	2.03×10^{8}	15,310,415	2,007,703	98,470	2.46×10^{8}	5.01926×10^{9}
8	923,531	1,019,204	3.89×10^{8}	23,755,102	517,251	54,974	1.37×10^{8}	1.29313×10^{9}
9	1,235,305	1,089,112	4.34×10^{8}	27,957,268	97,488	2,393	59,816,347	2.43721×10^{8}
10	460,469	587,716	2.81×10^{8}	7,587,528	12,487	5,693	14,233,174	3.12169×10^{7}
11	511,925	1,045,233	5.69×10^{8}	26,052,255	23,881	9,558	23,896,157	5.97016×10^{7}
12	618,583	867,063	5.24×10^{8}	18,078,548	37,053	13,444	33,609,508	9.26317×10^{7}
13	378,634	517,794	1.53×10^{8}	5,816,720	10,028	3,805	9,511,316	2.50696×10^{7}
14	201,055	442,160	1.36×10^{8}	7,137,129	8,464	4,433	11,081,853	2.11598×10^{7}
15	235,520	530,816	3.63×10^{8}	7,329,487	8,972	2,794	6,985,004	2.24290×10^{7}
16	1,741,301	1,768,088	9.09×10^{8}	74,164,151	16,438	5,501	13,753,187	4.10958×10^{7}
17	1,205,573	1,467,627	6.07×10^{8}	50,655,789	30,135	10,737	26,842,107	7.53363×10^{7}
18	267,142	648,736	3.46×10^{8}	10,889,741	9,387	3,861	9,653,349	2.34669×10^{7}
19	201,294	559,324	2.91×10^{8}	9,535,707	176,321	32,705	81,763,438	4.40804×10^{8}
20	1,004,395	1,029,941	4.51×10^{8}	23,474,508	7,456	3,283	8,207,169	1.86398×10^{7}
21	1,009,030	1,106,137	5.35×10^{8}	27,028,114	19,947	8,456	21,138,898	4.98680×10^{7}
22	1,026,085	1,252,659	3.07×10^{8}	41,767,584	15,567	5,151	12,878,350	3.89175×10^{7}
23	668,258	1,063,435	5.64×10^{8}	25,605,908	14,809	6,431	16,077,435	3.70216×10^{7}
24	1,024,237	1,451,561	6.14×10^{8}	50,648,927	9,298	3,252	8,130,340	2.32461×10^{7}
25	1,210,901	1,698,855	9.21×10^{8}	68,525,462	4,748	1,821	4,552,413	1.18697×10^{7}
26	269,741	793,744	5.32×10^{8}	17,351,838	5,026	1,852	4,629,178	1.25655×10^{7}
27	1,028,359	1,675,219	9.27×10^{8}	68,295,741	70,437	20,274	50,685,803	1.76093×10^{8}
28	900,507	986,915	4.31×10^{8}	22,348,311	384,134	47,109	1.18×10^{8}	9.60336×10^{8}
29	1,440,267	1,613,808	77,005,098	60,754,639	15,103	5,436	13,589,232	3.77577×10^{7}
30	1,000,210	944,963	3.51×10^{8}	20,113,584	10,216	3,513	8,783,479	2.55406×10^{7}
31	234,048	460,056	2.79×10^{8}	5,122,464	10,794	5,151	12,876,389	2.69844×10^{7}
32	513,937	1,128,749	6.77×10^{8}	31,275,619	10,690	5,008	12,520,770	2.67239×10^{7}
33	1,206,494	1,260,571	2.98×10^{8}	41,517,482	4,022	1,714	4,285,591	1.00541×10^{7}
34	919,073	949,681	3.06×10^{8}	21,349,023	46,521,698	400,260	1×10^{9}	1.16304×10^{11}
35	913,309	827,358	1.52×10^{8}	18,539,594	4,635	2,088	5,219,634	1.15883×10^{7}
36	1,731,266	1,284,105	2.8×10^{8}	46,045,343	37,843	12,454	31,134,289	9.46084×10^{7}
37	462,954	663,903	3.65×10^{8}	9,855,509	49,543	14,724	36,810,021	1.23858×10^{8}
38	379,715	657,659	3.4×10^{8}	9,344,743	17,334	6,787	16,967,552	4.33351×10^{7}
39	202,119	626,917	3.76×10^{8}	11,700,363	63,436	18,805	47,012,681	1.58591×10^{8}
40	510,661	951,599	4.43×10^{8}	21,220,494	9,488	4,749	11,872,844	2.37202×10^{7}

(*continued*)

Downloaded from http://iwaponline.com/wst/article-pdf/76/12/3410/241768/wst076123410.pdf
by guest

Table 4 | continued

	Electrical conductivity				pH			
Run	**ISE**	**IAE**	**ITAE**	**ITSE**	**ISE**	**IAE**	**ITAE**	**ITSE**
41	1,437,157	1,269,891	2.89×10^{8}	42,641,847	5,691	1,799	4,496,327	1.42287×10^{7}
42	907,191	1,182,746	6.66×10^{8}	32,721,414	6,244	2,915	7,287,334	1.56098×10^{7}
43	1,736,106	1,648,477	7.65×10^{8}	64,610,752	11,188	3,557	8,892,732	2.79702×10^{7}
44	899,118	809,116	1.96×10^{8}	16,794,890	5,912	2,139	5,346,795	1.47788×10^{7}
45	457,702	460,093	1.25×10^{8}	5,001,037	26,897	9,123	22,808,244	6.72417×10^{7}
46	381,604	738,891	4.42×10^{8}	12,520,367	4,737	2,514	6,285,632	1.18419×10^{7}
47	1,025,628	1,569,471	7.83×10^{8}	59,074,644	5,124	1,685	4,212,618	1.28089×10^{7}
48	466,067	730,653	4.36×10^{8}	12,262,724	3,407	1,575	3,937,538	8.51711×10^{6}
49	903,239	1,090,228	9×10^{8}	27,349,917	12,577	5,160	12,900,368	3.14429×10^{7}
50	995,999	798,612	1.65×10^{8}	16,260,456	6,884	2,252	5,630,256	1.72109×10^{7}
51	612,930	698,772	3.37×10^{8}	11,394,367	25,549	9,404	23,510,645	6.38730×10^{7}
52	268,359	725,999	4.47×10^{8}	14,013,836	4,013	1,961	4,902,727	1.00313×10^{7}
53	1,244,080	1,297,762	6.69×10^{8}	38,547,353	15,608	5,778	14,446,017	3.90189×10^{7}
54	383,737	810,740	5.27×10^{8}	15,907,816	3,588	1,864	4,659,720	8.96892×10^{6}
55	1,732,222	1,514,225	5.94×10^{8}	55,748,149	31,410	11,591	28,977,283	7.85248×10^{7}
56	671,238	1,150,868	6.71×10^{8}	30,903,431	19,173	8,098	20,245,634	4.79331×10^{7}
57	1,239,308	1,199,725	5.62×10^{8}	33,085,336	12,673	5,755	14,387,907	3.16822×10^{7}
58	232,942	339,429	1.23×10^{8}	2,645,051	7,379	2,710	6,774,356	1.84466×10^{7}
59	1,231,570	896,298	1.98×10^{8}	22,168,989	5,378	2,682	6,704,483	1.34454×10^{7}
60	610,775	543,579	1.48×10^{8}	7,740,158	11,887	4,620	11,550,995	2.97184×10^{7}
61	203,269	686,917	4.46×10^{8}	14,014,526	9,068	3,474	8,683,995	2.26704×10^{7}
62	511,242	792,151	2.11×10^{8}	15,993,465	7,863	2,560	6,400,572	1.96581×10^{7}
63	615,527	787,986	4.39×10^{8}	14,634,209	7,491	3,119	7,798,140	1.87272×10^{7}
64	237,457	594,217	4.34×10^{8}	9,682,667	15,532	6,834	17,085,817	3.88303×10^{7}

indicate good agreement between experimental data and estimated results as shown in Figure 3.

$$G_p(s)_{E.\ conductivity} = \frac{3.9818^{*}e^{-30s}}{0.000375\,s^3 + 19.3146\,s^2 + 248940s + 1} \quad (7)$$

$$G_p(s)_{pH} = \frac{-0.00148^{*}e^{-30s}}{0.1\,s^4 + 1.6\,s^3 + 6.1\,s^2 + s} \quad (8)$$

RSM was used as a new tuning method for optimizing PID parameters. Four level full factorial design matrices were formed for each controller and performance criteria values (ISE, IAE, ITAE, ITSE) of controllers were determined by applying the factors combinations, which were stated in the design matrices, to close-loop PID control simulations and presented in Table 4.

To describe the effects of PID parameters on the responses, ISE, IAE, ITAE and ITSE values were fitted to polynomial models in Equations (9)–(16) given in Tables 5 and 6.

The significance of the obtained models was examined by analysis of variance (ANOVA) with F test. The high F value shows a case where the variability of group means is large relative to the within group variability. Within group variation cannot be controlled, therefore the variation is due to individual differences (Moore 2007). If the model is statistically significant, F value of the model should be higher than the related F value given by the F distribution table. P value is also used to express the adequacy of the corresponding F value to imply the significance of the model. At 95% significance level, P value should be below 0.05. Determination coefficient (R^2) indicates the fit of the obtained model by comparing simulation results and

Downloaded from http://iwaponline.com/wst/article-pdf/76/12/3410/241768/wst076123410.pdf
by guest

Table 5 | Polynomial models of ISE, IAE, ITAE and ITSE for electrical conductivity

Polynomial model	Equation
$ISE = 6,004,051 - 9,369\,K_C - 478,596,905\,\tau_I - 51,777\,\tau_D + 5.834\,K_C^2 + 1,821,727,675,169\,\tau_I^2 + 662.3\,\tau_D^2 + 763,728\,K_C{*}\tau_I + 46.26\,K_C{*}\tau_D - 208,998\,\tau_I{*}\tau_D - 0.001232\,K_C^3 - 1,662,481,803,171,482\,\tau_I^3 + 5.89\,\tau_D^3 - 402\,K_C^2{*}\tau_I - 0.05335\,K_C^2{*}\tau_D - 1,681,161,326\,K_C{*}\tau_I^2 - 2,753\,K_C{*}\tau_I{*}\tau_D - 1.1317\,K_C{*}\tau_D^2 - 3,008,610,616\,\tau_I^2{*}\tau_D + 26,161\,\tau_I{*}\tau_D^2 + 0.085\,K_C^3{*}\tau_I + 0.000007\,K_C^3{*}\tau_D + 395,001\,K_C^2{*}\tau_I^2 - 0.96\,K_C^2{*}\tau_I{*}\tau_D + 0.001527\,K_C^2{*}\tau_D^2 + 970,727,619,047\,K_C{*}\tau_I^3 + 1,936,335\,K_C{*}\tau_I^2{*}\tau_D + 126\,K_C{*}\tau_I{*}\tau_D^2 - 0.01427\,K_C{*}\tau_D^3 + 1,675,174,602,935\,\tau_I^3{*}\tau_D - 45,046,980\,\tau_I^2{*}\tau_D^2 - 2,735\,\tau_I{*}\tau_D^3$	(9)
$IAE = 4,997,491 - 8,964\,K_C + 6,032,327,385\,\tau_I - 89,799\,\tau_D + 6.00\,K_C^2 - 5,172,383,573,333\,\tau_I^2 + 1,357\,\tau_D^2 - 3,509,085\,K_C{*}\tau_I + 274.1\,K_C{*}\tau_D - 40,505,568\,\tau_I{*}\tau_D - 0.001276\,K_C^3 + 1,527,978,577,795,560\,\tau_I^3 - 17.7\,\tau_D^3 + 436\,K_C^2{*}\tau_I - 0.2619\,K_C^2{*}\tau_D + 2,250,665,950\,K_C{*}\tau_I^2 + 2,940\,K_C{*}\tau_I{*}\tau_D - 2.49\,K_C{*}\tau_D^2 + 84,806,697,228\,\tau_I^2{*}\tau_D - 174,117\,\tau_I{*}\tau_D^2 + 0.06\,K_C^3{*}\tau_I + 0.000057\,K_C^3{*}\tau_D - 152,772\,K_C^2{*}\tau_I^2 + 26.9\,K_C^2{*}\tau_I{*}\tau_D + 0.002582\,K_C^2{*}\tau_D^2 - 374,148,571,441\,K_C{*}\tau_I^3 - 32,539,304\,K_C{*}\tau_I^2{*}\tau_D - 1,616\,K_C{*}\tau_I{*}\tau_D^2 - 0.0134\,K_C{*}\tau_D^3 - 48,309,587,302,165\,\tau_I^3{*}\tau_D - 437,156,261\,\tau_I^2{*}\tau_D^2 + 55,511\,\tau_I{*}\tau_D^3$	(10)
$ITAE = -221,820,386 - 1,041,590\,K_C + 36,931,047,320,330\,\tau_I - 108,783,477\,\tau_D + 721\,K_C^2 - 349,977,062,891,640,580\,\tau_I^2 + 12,246,651\,\tau_D^2 - 3,229,215,864\,K_c{*}\tau_I + 149,042\,K_C{*}\tau_D - 644,311,458,070\,\tau_I{*}\tau_D + 0.06\,K_C^3 + 976,567,527,256,254,840,000\,\tau_I^3 - 272,421\,\tau_D^3 - 15,960,477\,K_C^2{*}\tau_I + 2\,K_C^2{*}\tau_D + 180,766,587,793,385\,K_C{*}\tau_I^2 - 169,268,870\,K_C{*}\tau_I{*}\tau_D - 15,265\,K_C{*}\tau_D^2 + 3,288,451,917,771,136\,\tau_I^2{*}\tau_D + 34,134,607,685\,\tau_I{*}\tau_D^2 + 1,789\,K_C^3{*}\tau_I - 0.023\,K_C^3{*}\tau_D + 36,712,111,129\,K_C^2{*}\tau_I^2 + 66,950\,K_C^2{*}\tau_I{*}\tau_D + 3.26\,K_C^2{*}\tau_D^2 - 667,099,507,116,159,100\,K_C{*}\tau_I^3 + 608,664,555,277\,K_C{*}\tau_I^2{*}\tau_D - 7,165,803\,K_C{*}\tau_I{*}\tau_D^2 + 242\,K_C{*}\tau_D^3 - 7,429,308,820,063,724,500\,\tau_I^3{*}\tau_D - 43,664,367,074,504\,\tau_I^2{*}\tau_D^2 - 377,446,431\,\tau_I{*}\tau_D^3$	(11)
$ITSE = 304,286,983 - 614,399\,K_C + 382,105,586,939\,\tau_I - 1,510,086\,\tau_D + 428.3\,K_C^2 + 1,950,226,906,340,675\,\tau_I^2 + 24,419\,\tau_D^2 - 963,699,913\,K_C{*}\tau_I + 3,612\,K_C{*}\tau_D - 1,554,451,687\,\tau_I{*}\tau_D - 0.09737K_C^3 - 2,279,942,547,047,112,700\,\tau_I^3 + 1,146\,\tau_D^3 + 798,152\,K_C^2{*}\tau_I - 3.465\,K_C^2{*}\tau_D - 1,844,525,399,862\,K_C{*}\tau_I^2 + 1,437,683\,K_C{*}\tau_I{*}\tau_D - 71.40\,K_C{*}\tau_D^2 + 1,520,819,335,157\,\tau_I^2{*}\tau_D + 5,610,807\,\tau_I{*}\tau_D^2 - 212.8\,K_C^3{*}\tau_I + 0.000343\,K_C^3{*}\tau_D + 436,889,853\,K_C^2{*}\tau_I^2 - 502\,K_C^2{*}\tau_I{*}\tau_D + 0.09742\,K_C^2{*}\tau_D^2 + 1,358,532,891,428,281\,K_C{*}\tau_I^3 - 845,351,376\,K_C{*}\tau_I^2{*}\tau_D + 7,627K_C{*}\tau_I{*}\tau_D^2 - 1.884\,K_C{*}\tau_D^3 - 105,843,809,542,828\,\tau_I^3{*}\tau_D - 2,364,832,757\,\tau_I^2{*}\tau_D^2 - 247,911\,\tau_I{*}\tau_D^3$	(12)

predicted data. While R^2 provides an estimate of the strength of the relationship between the model and the response variable, it does not provide a formal hypothesis test for this relationship. The overall F test determines whether this relationship is statistically significant or not. If the P value for the overall F test is less than the specified significance level, it can be concluded that the R^2 value is significantly different from zero (Moore 2007). Results of ANOVA for electrical conductivity and pH processes are shown in Table 7.

In Table 7, F values are higher than the tabulated one ($F_{0.05(31,32)} = 1.8295$) at 95% confidence level, which

Downloaded from http://iwaponline.com/wst/article-pdf/76/12/3410/241768/wst076123410.pdf
by guest

Table 6 | Polynomial models of ISE, IAE, ITAE and ITSE for pH

Polynomial model	Equation
$ISE = -14,628,709 - 2,083,823K_C - 349,539,009\,\tau_I + 716,747\,\tau_D - 622,119\,K_C^2 - 5,573,537,183\,\tau_I^2 - 11,828\,\tau_D^2 - 979,115,480\,K_C{*}\tau_I + 127,629\,K_c{*}\tau_D - 32,065,482\,\tau_I{*}\tau_D - 53,452\,K_C^3 + 524,609,033,203\,\tau_I^3 + 172\,\tau_D^3 - 151,961,809\,K_C^2{*}\tau_I + 29,167\,K_C^2{*}\tau_D + 39,848,794,238\,K_C{*}\tau_I^2 - 11,991,925\,K_C{*}\tau_I{*}\tau_D + 1,266\,K_C{*}\tau_D^2 + 1,923,175,434\,\tau_I^2{*}\tau_D - 314,152\,\tau_I{*}\tau_D^2 - 8,170,932\,K_C^3{*}\tau_I + 2,599\,K_C^3{*}\tau_D + 2,730,224,976\,K_C^2{*}\tau_I^2 - 1,249,407\,K_C^2{*}\tau_I{*}\tau_D + 274\,K_C^2{*}\tau_D^2 - 578,331,722,005\,K_C{*}\tau_I^3 + 330,736,375\,K_C{*}\tau_I^2{*}\tau_D - 104,442\,K_C{*}\tau_I{*}\tau_D^2 + 18.2\,K_C{*}\tau_D^3 - 47,808,933,594\,\tau_I^3{*}\tau_D + 18,836,179\,\tau_I^2{*}\,\tau_D^2 - 4,719\,\tau_I{*}\tau_D^3$	(13)
$IAE = -100,478 + 1,861K_C + 445,457\,\tau_I + 6,187\,\tau_D - 788\,K_C^2 - 281,997,424\,\tau_I^2 - 97\,\tau_D^2 - 7,898,712K_C{*}\tau_I + 1,158K_C{*}\tau_D - 266,927\,\tau_I{*}\tau_D - 133\,K_C^3 + 9,536,645,508\,\tau_I^3 + 1.268\,\tau_D^3 - 1,166,917K_C^2{*}\tau_I + 202\,K_C^2{*}\tau_D + 320,621,777\,K_C{*}\tau_I^2 - 85,157\,K_C{*}\tau_I{*}\tau_D + 4.9\,K_C{*}\tau_D^2 + 17,245,495\,\tau_I^2{*}\tau_D - 2,385\,\tau_I{*}\tau_D^2 - 59,260\,K_C^3{*}\tau_I + 15.1\,K_C^3{*}\tau_D + 20,679,993K_C^2{*}\tau_I^2 - 8,331\,K_C^2{*}\tau_I{*}\tau_D + 1.44\,K_C^2{*}\tau_D^2 - 5,171,870,931\,K_C{*}\tau_I^3 + 2,787,649\,K_C{*}\tau_I^2{*}\tau_D - 795\,K_C{*}\tau_I{*}\tau_D^2 + 0.122\,K_C{*}\tau_D^3 - 471,806,315\,\tau_I^3{*}\tau_D + 173,341\,\tau_I^2{*}\,\tau_D^2 - 40.4\,\tau_I{*}\tau_D^3$	(14)
$ITAE = -232,116,736 - 4,231,567\,K_C + 9,696,599,832\,\tau_I + 10,808,622\,\tau_D - 4,916,639\,K_C^2 - 930,492,116,150\,\tau_I^2 - 174,981\,\tau_D^2 - 15,726,440,398\,K_C{*}\tau_I + 1,823,493\,K_C{*}\tau_D - 613,287,311\,\tau_I{*}\tau_D - 543,776\,K_C^3 + 24,719,786,490,886\,\tau_I^3 + 2,826\,\tau_D^3 - 2,281,149,864\,K_C^2{*}\tau_I + 395,613\,K_C^2{*}\tau_D + 769,998,188,965\,K_C{*}\tau_I^2 - 213,160,656\,K_C{*}\tau_I{*}\tau_D + 19,821\,K_C{*}\tau_D^2 + 46,835,590,954\,\tau_I^2{*}\tau_D - 8,108,200\,\tau_I{*}\tau_D^2 - 116,606,368\,K_C^3{*}\tau_I + 34,368\,K_C^3{*}\tau_D + 48,414,237,000\,K_C^2{*}\tau_I^2 - 20,321,946\,K_C^2{*}\tau_I{*}\tau_D + 3,941\,K_C^2{*}\tau_D^2 - 13,148,491,076,660\,K_C{*}\tau_I^3 + 7,011,161,445\,K_C{*}\tau_I^2{*}\tau_D - 1,947,882\,K_C{*}\tau_I{*}\tau_D^2 + 285\,K_C{*}\tau_D^3 - 1,197,045,425,456\,\tau_I^3{*}\tau_D + 412,327,029\,\tau_I^2{*}\,\tau_D^2 - 84,765\,\tau_I{*}\tau_D^3$	(15)
$ITSE = -36,571,773,870 - 5,209,560,308\,K_C - 873,847,518,308\,\tau_I + 1,791,867,530\,\tau_D - 1,555,299,660\,K_C^2 - 13,933,837,299,350\,\tau_I^2 - 29,569,069\,\tau_D^2 - 2,447,788,805,059\,K_C{*}\tau_I + 319,073,019\,K_C{*}\tau_D - 80,163,714,555\,\tau_I{*}\tau_D - 133,630,859\,K_C^3 + 1,311,522,468,391,986\,\tau_I^3 + 430,619\,\tau_D^3 - 379,904,523,931\,K_C^2{*}\tau_I + 72,917,083\,K_C^2{*}\tau_D + 99,621,991,588,966\,K_C{*}\tau_I^2 - 29,979,811,464\,K_C{*}\tau_I{*}\tau_D + 3,164,376\,K_C{*}\tau_D^2 + 4,807,939,153,774\,\tau_I^2{*}\tau_D - 785,379,786\,\tau_I{*}\tau_D^2 - 20,427,330,150\,K_C^3{*}\tau_I + 6,497,733\,K_C^3{*}\tau_D + 6,825,562,355,102\,K_C^2{*}\tau_I^2 - 3,123,517,540\,K_C^2{*}\tau_I{*}\tau_D + 685,462\,K_C^2{*}\tau_D^2 - 1,445,829,391,796,917\,K_C{*}\tau_I^3 + 826,840,911,497\,K_C{*}\tau_I^2{*}\tau_D - 261,104,037\,K_C{*}\tau_I{*}\tau_D^2 + 45,559\,K_C{*}\tau_D^3 - 119,522,341,419,273\,\tau_I^3{*}\tau_D + 47,090,445,241\,\tau_I^2{*}\,\tau_D^2 - 11,797,874\,\tau_I{*}\tau_D^3$	(16)

indicates the statistical significance of the models. Obtaining large F values shows that the terms in the regression model have meaningful effects, but it also shows how little random errors play a role in the consistency of the pattern obtained at the same time (Moore 2007). Significance of the models can also be verified by corresponding P values, which are all zero to three decimal places. Determination coefficients show that suggested models explain more than 80% of the total variation, which means a good enough fit to express the design range.

The effects of PID parameters on performance criteria were visualized and shown in the figures given in Appendices 1 and 2 (available with the online version of this paper).

Downloaded from http://iwaponline.com/wst/article-pdf/76/12/3410/241768/wst076123410.pdf
by guest

Table 7 | ANOVA results for electrical conductivity and pH

		Electrical conductivity					pH				
	Source	Degrees of freedom	Adj. sum of squares	Adj. mean square	F	P	Degrees of freedom	Adj. sum of squares	Adj. mean square	F	P
ISE	Model	31	1.26×10^{13}	4.06×10^{11}	403,891.07	0.000	31	1.74×10^{15}	5.60×10^{13}	4.56	0.000
	Error	32	3.21×10^{7}	1.00×10^{6}			32	3.93×10^{14}	1.23×10^{13}		
	Total	63	1.26×10^{13}				63	2.13×10^{15}			
		$R^2 = 100.00$ Adj. $R^2 = 100.00$					$R^2 = 81.55$ Adj. $R^2 = 63.67$				
IAE	Model	31	8.98×10^{12}	2.90×10^{11}	2,433.60	0.000	31	1.49×10^{11}	4.80×10^{9}	9.74	0.000
	Error	32	3.81×10^{9}	1.19×10^{8}			32	1.58×10^{10}	4.93×10^{8}		
	Total	63	8.98×10^{12}				63	1.65×10^{11}			
		$R^2 = 99.96$ Adj. $R^2 = 99.92$					$R^2 = 90.42$ Adj. $R^2 = 81.14$				
ITAE	Model	31	2.67×10^{18}	8.60×10^{16}	9.56	0.000	31	9.29×10^{17}	2.99×10^{16}	9.72	0.000
	Error	32	2.88×10^{17}	8.99×10^{15}			32	9.87×10^{16}	3.08×10^{15}		
	Total	63	2.95×10^{18}				63	1.03×10^{18}			
		$R^2 = 90.25$ Adj. $R^2 = 80.81$					$R^2 = 90.40$ Adj. $R^2 = 81.09$				
ITSE	Model	31	2.38×10^{16}	7.69×10^{14}	94,415.76	0.000	31	1.08×10^{22}	3.50×10^{20}	4.56	0.000
	Error	32	2.61×10^{11}	8.14×10^{9}			32	2.46×10^{21}	7.67×10^{19}		
	Total	63	2.38×10^{16}				63	1.33×10^{22}			
		$R^2 = 100.00$ Adj. $R^2 = 100.00$					$R^2 = 81.55$ Adj. $R^2 = 63.67$				

Multi-objective optimization was achieved successfully through overall multi-desirability function which minimizes controller performance criteria ISE, IAE, ITAE and ITSE simultaneously to determine the optimum values of PID controller parameters, K_C, τ_I and τ_D. Depending on the response surface models, K_C, τ_I and τ_D were optimized by using MINITAB 17 software to provide minimum values of ISE, IAE, ITAE and ITSE for the highest overall desirability as shown in Table 8. The optimization numerically determines a point that maximizes the desirability function to 1. For multiple responses, all goals with equal weightage were combined into one desirability function. For multi-response optimization, each response must have low and high limits assigned to each objective (Aggarwal *et al.* 2008). Overall multi-desirabilities of 0.9880 and 1.000 were achieved for electrical conductivity and pH controllers respectively.

The results indicate that minimum performance criteria along with maximum controller performance goals can be achieved with high values of K_C, very low values of τ_I and mid range values of τ_D for electrical conductivity. Similarly, optimum pH control can be achieved with low values of K_C, mid-range values of τ_I and high values of τ_D. A negative K_C value indicates that inverted control action is required to control pH. Theoretical control was utilized to examine the performance of optimum PID parameters which were obtained by using MINITAB. Electrical conductivity, pH responses and related manipulated variables change with time under theoretical control using optimum PID parameters are presented in Appendix 3 (available with the online version of this paper). In the electrical conductivity process, minimum ISE, IAE, ITAE and ITSE values were found to be 212,075, 272,514, 19,552,588 and 2,387,453 respectively. In the pH process, minimum performance criteria values obtained were 11,089, 3,721, 898,180 and 1,558,913 for ISE, IAE, ITAE and ITSE respectively. Theoretically optimized controller performances were compared with three different tuning methods (Cohen–Coon (Cohen & Coon 1953), Ziegler–Nichols (Ziegler & Nichols 1942) and CST) and the results are given in Table 9.

Since the RSM tuning method enables the lower values of ISE, IAE, ITAE and ITSE rather than only one criteria, which becomes an indicator of better performance, RSM has increased controller performance in terms of ISE as 99.78%, 99.78% and 99.85% for electrical conductivity, 75.98%, 78.27% and 75.91% for pH compared with

Table 8 | Optimization of PID parameters

Process	Optimum values			Overall desirability
	K_C (s)	τ_I (s)	τ_D (s)	
Electrical conductivity	1,500.00000	0.0000	16.4636	0.9880
pH	−8.6970	0.0211	50.0000	1.0000

Downloaded from http://iwaponline.com/wst/article-pdf/76/12/3410/241768/wst076123410.pdf
by guest

Table 9 | Comparison of different PID tuning methods for electrical conductivity and pH control performances

Parameter	Tuning method	ISE	IAE	ITAE	ITSE
Electrical conductivity	RSM	212,075	272,514	19,552,588	2,387,453
	Cohen–Coon	96,639,597	42,826,454	48,766,452,368	100,140,713,172
	Ziegler–Nichols	97,806,497	43,114,500	49,246,201,374	102,004,824,881
	CST	141,552,681	52,438,296	65,380,887,625	1,760,394,219
pH	RSM	11,089	3,721	898,180	1,558,913
	Cohen–Coon	46,158	16,194	17,164,241	39,618,112
	Ziegler–Nichols	51,029	16,920	17,576,047	44,042,326
	CST	46,023	16,165	17,158,498	39,602,857

Cohen–Coon, Ziegler–Nichols and CST respectively. Results show that a significant performance improvement was achieved by using this method compared to previous literature. The applicability of RSM for tuning the controllers of industrial wastewater treatment processes is extremely high. Similar to work already published, all that is needed to implement this method is either dynamic analysis data or a mathematical model that describes the system. Similarly, since the optimization is performed in a simulation environment, there will not be any application cost.

As can be seen from Appendix 3, control applications of electrical conductivity and pH processes were successfully achieved theoretically. Before applying optimum theoretical PID parameters to the experimental process, a

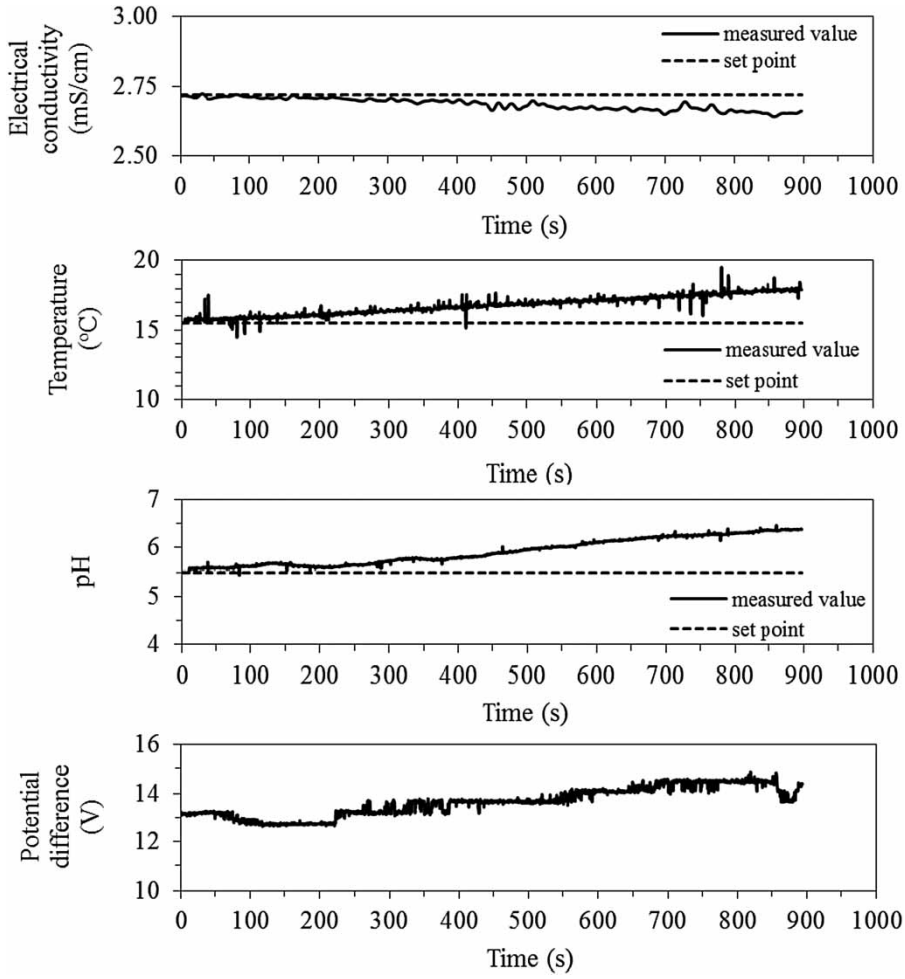

Figure 4 | Variations of treatment variables of pulp and paper mill wastewater under uncontrolled conditions.

Downloaded from http://iwaponline.com/wst/article-pdf/76/12/3410/241768/wst076123410.pdf
by guest

study without control was carried out to compare the results with controlled conditions with respect to pollutant removal and energy consumption. The variation of electrical conductivity, pH, temperature and potential difference with time are given in Figure 4. It is clearly shown in Figure 4 that electrical conductivity was reduced by 0.08 mS/cm while temperature, pH and potential difference increased by 2.43 °C, 0.88 units and 1.16 V during 15 min of treatment.

The first experimental control was performed for single input–single output (SISO) electrical conductivity under 15 °C constant temperature using optimum PID parameters. Control results of SISO electrical conductivity are shown in Figure 5. Uncontrolled pH was increased by 0.7 units in this experiment. It can be seen from the figure that optimum PID parameters successfully controlled electrical conductivity at a desired value of 2.72 mS/cm. Potential difference decreased with the control of electrical

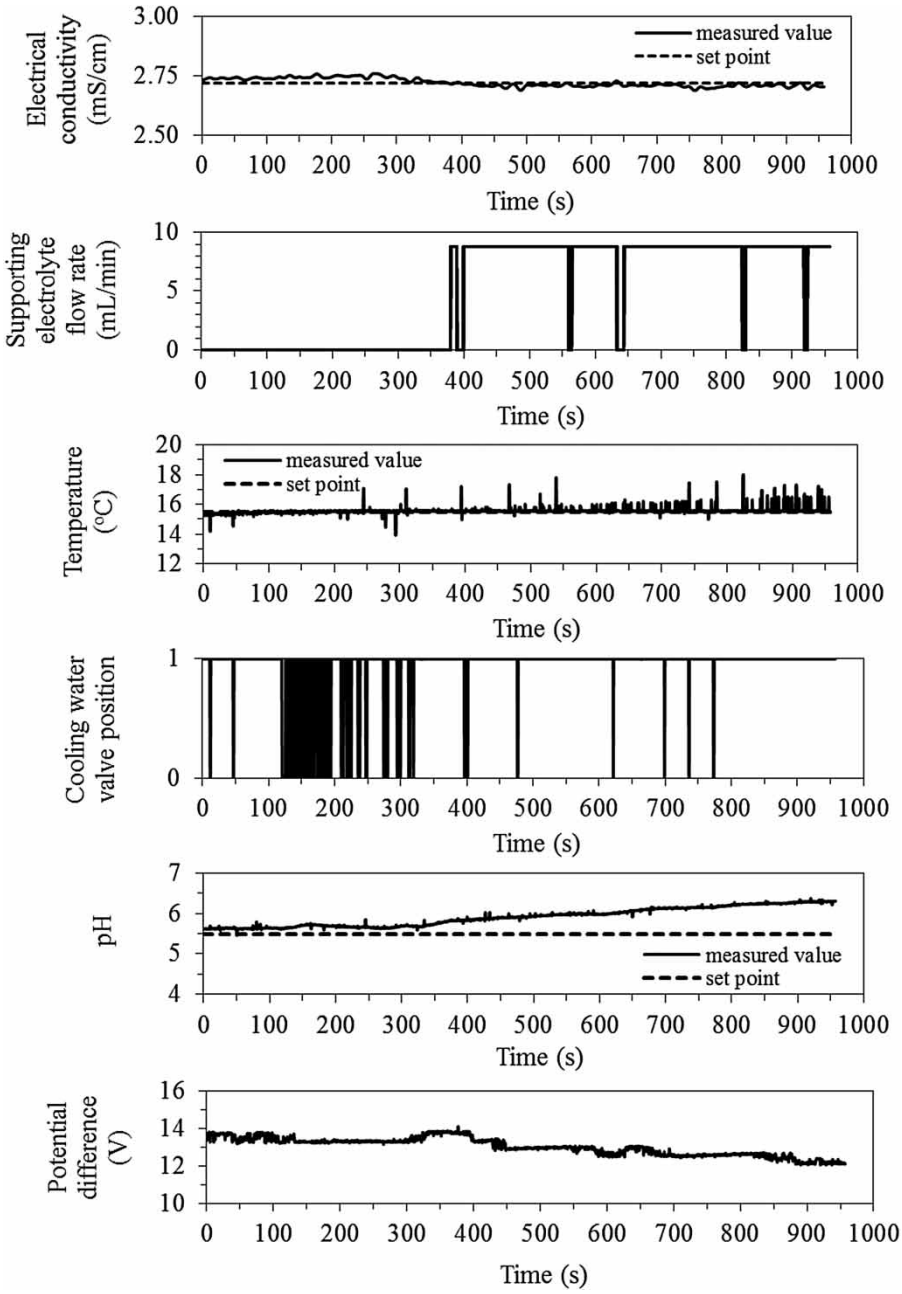

Figure 5 | Variations of treatment variables of pulp and paper mill wastewater under SISO controlled electrical conductivity case ($K_C = 1{,}500$ s, $\tau_I = 0$ s, $\tau_D = 16.46$ s).

Downloaded from http://iwaponline.com/wst/article-pdf/76/12/3410/241768/wst076123410.pdf
by guest

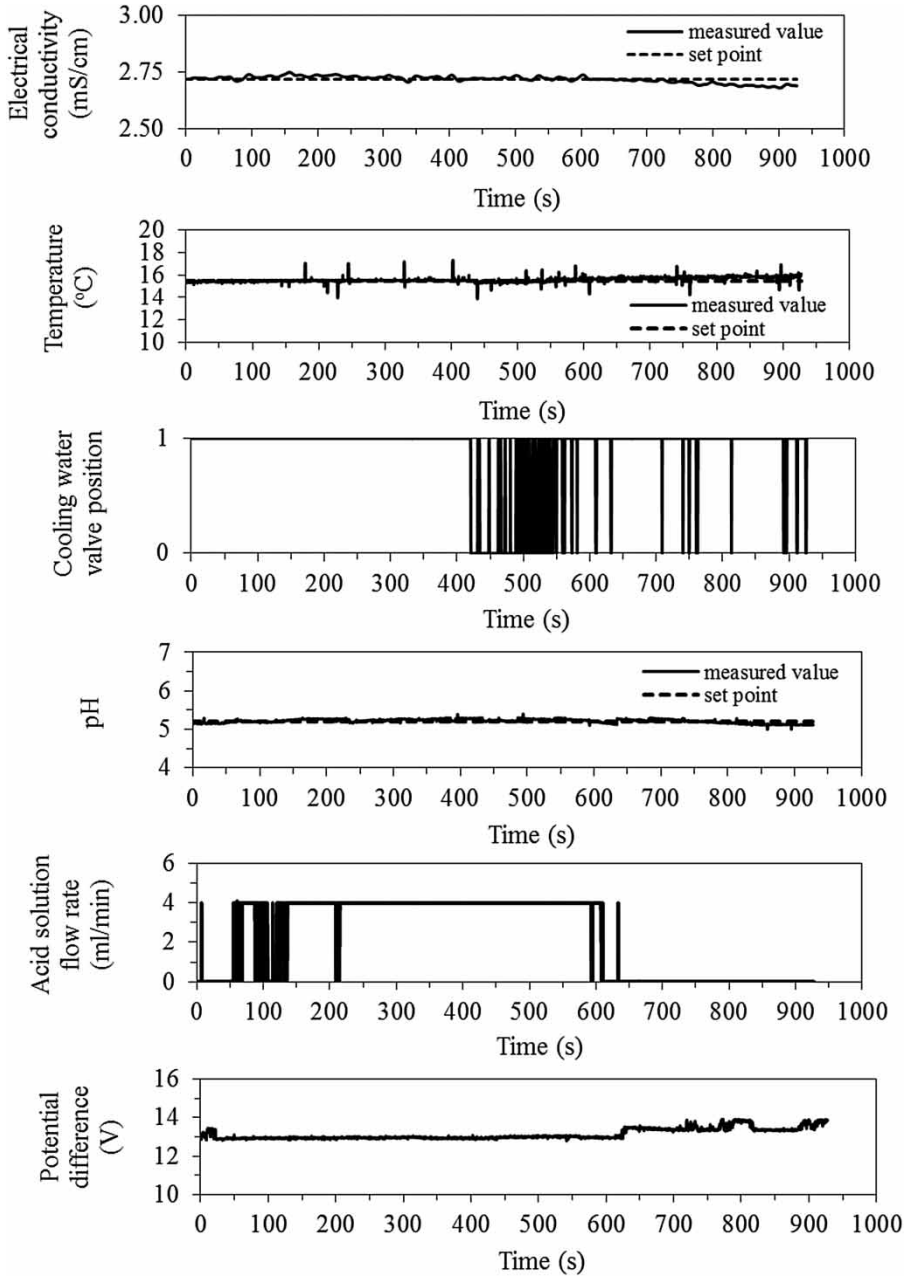

Figure 6 | Variations of treatment variables of pulp and paper mill wastewater under SISO pH controlled case ($K_C = -8.69$ s, $\tau_I = 0.0211$ s, $\tau_D = 50$ s).

conductivity. ISE, IAE, ITAE and ITSE values were found as 0.6048, 28.8251, 11,171 and 195 respectively.

SISO pH control application was performed experimentally under 15 °C constant temperature and results are given in Figure 6. Uncontrolled electrical conductivity was decreased as 0.04 mS/cm due to chlorine formation under uncontrolled conditions. This reduction was 50% lower than the fully uncontrolled process. Acid solution addition for pH control aided electrical conductivity as a supporting electrolyte during treatment. According to the results, SISO pH was successfully controlled with optimum PID parameters which were obtained theoretically. ISE, IAE, ITAE and ITSE values obtained were 5.2727, 84.6328, 41,914 and 2,721 respectively.

Multi input–multi output control (MIMO) of electrical conductivity, pH and temperature were carried out experimentally. Variations of the manipulated variables, controlled variables and potential difference with time are presented in Figure 7. ISE, IAE, ITAE and ITSE values were calculated as 0.272, 17.1192, 6,665 and 91.0554 for

Downloaded from http://iwaponline.com/wst/article-pdf/76/12/3410/241768/wst076123410.pdf
by guest

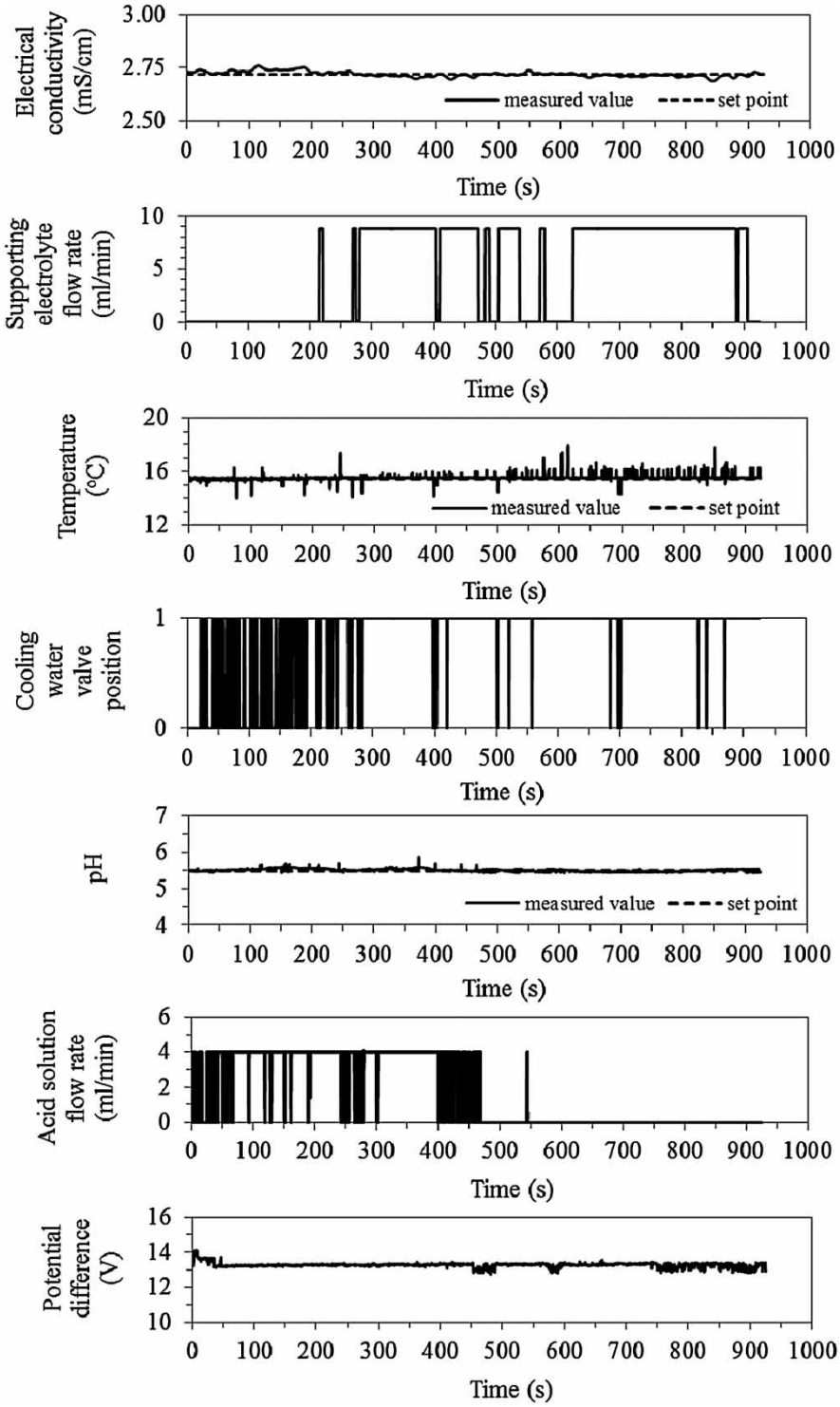

Figure 7 | Variations of treatment variables of pulp and paper mill wastewater under MIMO control of electrical conductivity and pH ($K_C = 1{,}500$ s, $\tau_I = 0$ s, $\tau_D = 16.46$ s for electrical conductivity, $K_C = -8.69$ s, $\tau_I = 0.0211$ s, $\tau_D = 50$ s for pH).

electrical conductivity; 3.7918, 65.2707, 27,310 and 1,340 for pH processes. MIMO performance criteria values were compared with SISO electrical conductivity and SISO pH control applications and results revealed that MIMO control reduced performance criteria values and showed better performance due to synergistic action of controllers.

Downloaded from http://iwaponline.com/wst/article-pdf/76/12/3410/241768/wst076123410.pdf
by guest

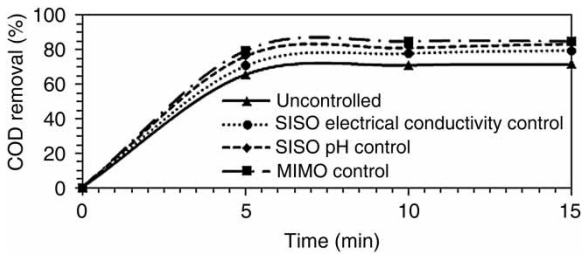

Figure 8 | Variation of COD values with time for different treatment methods.

Table 10 | Pollutant removal and energy consumption values for different types of treatment

Treatment	COD removal (%)	Colour removal (%)	Turbidity removal (%)	Energy consumption (kWh/m^3)
Uncontrolled	71.9	97.12	99.4	4.14
SISO electrical conductivity control	79.6	99.5	99.7	3.86
SISO pH control	83.8	98.8	99.3	4.10
MIMO control	85	99.04	99.6	3.87

Variations of COD values with time were determined and are shown in Figure 8. It can be concluded from the figure that MIMO control implied maximum COD removal at 7 min of treatment. pH controlled treatment showed a COD value close to MIMO treatment at the end of 15 min. This result revealed that pH is one of the most effective parameters on COD removal in an EC process since monomeric and several polymeric hydroxo species may form at an appropriate pH of the solution (Solak *et al.* 2009).

Experimental studies were compared with respect to COD, colour and turbidity removal percentages and energy consumption. It can be seen from Table 10 that MIMO control provided maximum COD removal, whereas minimum energy consumption was achieved with SISO electrical conductivity control.

Table 11 shows the comparison of obtained results with the previously published studies. Katal & Pahlavanzadeh (2011) applied EC to paper mill wastewater to investigate the effects of operating parameters. According to the results, during 30 min of treatment 78% COD and 95% colour removal was reached at pH 6 with 70 mA/cm^2 current density. Sridhar *et al.* (2011) studied optimum process conditions of bleaching effluent through EC and observed a COD removal of 85% and a colour removal of 90% under the conditions of 15 mA/cm^2, pH 6 and 30 min. Aghdam *et al.* (2016) achieved removal efficiencies of 83% and 91% for COD and colour respectively, at pH 8 for 60 min of treatment under 6.167 mA/cm^2. Asaithambi (2016) reported a reduction of 70% COD and an energy consumption of 4.4 kWh/m^3 in pulp and paper mill wastewater treatment under conditions of 120 min electrolysis time, 0.40 A/dm^2 current density and initial pH 6. In this study, 85% COD and 99.04% colour removal was observed at pH 5.82 using PID controlled EC treatment. The result of this study was found to be compatible with previously published work in terms of pollutant removal and energy consumption.

Table 11 | Comparison of results with the similar studies in the literature

Reference	Operating parameters	Operating conditions	Anode-cathode	Pollutant removal (%)	Energy consumption
Katal & Pahlavanzadeh (2011)	Electrolysis time Current density Initial pH	30 min 70 mA/cm^2 6	Al-Al	~% 78 COD ~% 95 colour	–
Sridhar *et al.* (2011)	Electrolysis time Current density Initial pH	30 min 15 mA/cm^2 6	Al-Al	~% 85 COD ~% 90 colour	–
Aghdam *et al.* (2016)	Electrolysis time Current density Initial pH	60 min 4.167 mA/cm^2 6	Fe-Al	~% 83 COD ~% 91 colour	–
Asaithambi (2016)	Electrolysis time Current density Initial pH	120 min 0.40 A/dm^2 6	Fe-Fe	~% 70 COD	4.4 kWh/m^3
This study	Electrolysis time Current density pH	15 min 6.78 mA/cm^2 5.82	Al-Al	% 85 COD % 99.04 colour	3.87 kWh/m^3

Downloaded from http://iwaponline.com/wst/article-pdf/76/12/3410/241768/wst076123410.pdf
by guest

CONCLUSIONS

In this work, the performance of a new PID parameter tuning method was evaluated. The results indicate that the controller tuned using RSM performs much better than the controllers tuned with CST in MATLAB, and the conventional tuning methods of Cohen–Coon and Ziegler–Nichols. SISO electrical conductivity, SISO pH and MIMO control studies were carried out experimentally by using theoretically optimized PID parameters and performance of the controllers were found satisfactory. MIMO control application showed minimum performance criteria values and this result indicated that there is synergistic interaction between electrical conductivity and pH controllers. Pollutant removal and energy consumption values of the control studies were compared with uncontrolled treatment. According to the results, SISO electrical conductivity control decreased energy consumption and SISO pH control was evaluated to be effective in COD removal. Compared with uncontrolled treatment, SISO electrical conductivity, SISO pH and MIMO control applications increased COD removal by 10.71%, 16.55%, 18.22% respectively. Colour and turbidity removal percentages were above 97% and almost the same for all types of experiment performed in this study and this result is related to EC, which is an effective treatment method for removing even the smallest colloidal particles that cause turbidity and colour problems in wastewater. As a conclusion RSM can effectively be used for PID parameter tuning as a new method. Enhancement of pollutant removal and decrease in energy consumption goals were achieved with MIMO control, which made the EC process more applicable.

ACKNOWLEDGEMENT

This work was supported by Ankara University Scientific Research Projects Coordination Unit [grant numbers 14L0443001, 14L0443005 and 16B0443001].

REFERENCES

Abbas, A. 1997 A new set of controller tuning relations. *ISA Transactions* **36** (3), 183–187.

Aggarwal, A., Singh, H., Kumar, P. & Singh, M. 2008 Optimization of multiple quality characteristics for CNC turning under cryogenic cutting environment using desirability function. *Journal of Materials Processing Technology* **205** (1), 42–50.

Aghdam, M. A., Karimina, H. R. & Safari, S. 2016 Removal of lignin, COD, and color from pulp and paper wastewater using electrocoagulation. *Desalination and Water Treatment* **52** (21), 9698–9704.

Alinsafi, A., Khemis, M., Pons, M. N., Leclerc, J. P., Yaacoubi, A., Benhammou, A. & Nejmeddine, A. 2005 Electrocoagulation of reactive textile dyes and textile wastewater. *Chemical Engineering and Processing: Process Intensification* **44** (4), 461–470.

Altinten, A., Erdogan, S., Alioglu, F., Hapoglu, H. & Alpbaz, M. 2004 Application of adaptive PID control with genetic algorithm to a polymerization reactor. *Chemical Engineering Communications* **191** (9), 1158–1172.

Altuntaş, S. & Hapoğlu, H. 2016 Control of adiabatic continuous stirred tank reactor at an unstable operating point. *Bulgarian Chemical Communications* **48** (C), 14–19.

Ang, K. H., Chong, G. & Li, Y. 2005 PID control system analysis, design, and technology. *IEEE Transactions on Control Systems Technology* **13** (4), 559–576.

APHA/AWWA/WEF 2005 *Standard Methods for the Examination of Water and Wastewater*, 21st edn. American Public Health Association/American Water Works Association/Water Environment Federation, Washington, DC, USA.

Asaithambi, P. 2016 Studies on various operating parameters for the removal of COD from pulp and paper industry using electrocoagulation process. *Desalination and Water Treatment* **57** (25), 11746–11755.

Astrom, K. J., Hagglund, T., Hang, C. C. & Ho, W. K. 1993 Automatic tuning and adaptation for PID controllers–A survey. *Control Engineering Practice* **1** (4), 699–714.

Bayramoglu, M., Kobya, M., Can, O. T. & Sozbir, M. 2004 Operating cost analysis of electrocoagulation of textile dye wastewater. *Separation and Purification Technology* **37** (2), 117–125.

Behrooz, R., Abadi, H. H. & Mohebby, B. 2011 Turbidity and BOD removal of a paper recycling mill effluent by electrocoagulation technique. *Desalination and Water Treatment* **28** (1–3), 65–68.

Benaissa, F., Kermet-Said, H. & Moulai-Mostefa, N. 2016 Optimization and kinetic modeling of electrocoagulation treatment of dairy wastewater. *Desalination and Water Treatment* **57** (13), 5988–5994.

Camcioglu, S., Pekel, L. C., Polat, K. & Hapoglu, H. 2014 Experimental design of wastewater treatment with electrocoagulation. *Management of Environmental Quality: An International Journal* **25** (1), 86–95.

Camcıoğlu, Ş., Özyurt, B., Zeybek, Z. & Hapoğlu, H. 2016 Experimental application of one step ahead advanced pH control to water-based paint wastewater treatment. *Journal of the Faculty of Engineering and Architecture of Gazi University* **31** (3), 655–664.

Cañizares, P., Carmona, M., Lobato, J., Martínez, F. & Rodrigo, M. 2005 Electrodissolution of aluminum electrodes in electrocoagulation processes. *Industrial & Engineering Chemistry Research* **44** (12), 4178–4185.

Cohen, G. & Coon, G. A. 1953 Theoretical consideration of retarded control. *Transactions of ASME* **75** (1), 827–834.

Cominos, P. & Munro, N. 2002 PID controllers: recent tuning methods and design to specification. *IEE Proceedings-Control Theory and Applications* **149** (1), 46–53.

Downloaded from http://iwaponline.com/wst/article-pdf/76/12/3410/241768/wst076123410.pdf
by guest

Demirci, Y., Pekel, L., Altınten, A. & Alpbaz, M. 2015 Application of fuzzy control on the electrocoagulation process to treat textile wastewater. *Environmental Technology* **36** (24), 3243–3252.

El-Ashtoukhy, E., Amin, N. & Abdelwahab, O. 2009 Treatment of paper mill effluents in a batch-stirred electrochemical tank reactor. *Chemical Engineering Journal* **146** (2), 205–210.

Hang, C. C., Astrom, K. J. & Ho, W. K. 1991 Refinements of the Ziegler-Nichols tuning formula. *IEE Proceedings D Control Theory and Applications* **138** (2), 111–118.

Hassan, M. M. & Hawkyard, C. J. 2002 Decolourisation of aqueous dyes by sequential oxidation treatment with ozone and Fenton's reagent. *Journal of Chemical Technology and Biotechnology* **77** (7), 834–841.

Karacan, S., Hapoglu, H., Cabbar, Y. & Alpbaz, M. 1997 Pole placement self tuning control for packed distillation column. *Chemical Engineering and Processing: Process Intensification* **36** (4), 309–315.

Katal, R. & Pahlavanzadeh, H. 2011 Influence of different combinations of aluminum and iron electrode on electrocoagulation efficiency: application to the treatment of paper mill wastewater. *Desalination* **265** (1), 199–205.

Liu, X., Shi, Y. & Xu, J. 2017 Parameters tuning approach for proportion integration differentiation controller of magnetorheological fluids brake based on improved fruit fly optimization algorithm. *Symmetry* **9** (7), 109.

Mahmoodi, N. M. & Dalvand, A. 2013 Treatment of colored textile wastewater containing acid dye using electrocoagulation process. *Desalination and Water Treatment* **51** (31–33), 5959–5964.

McCleskey, R., Nordstrom, D., Ryan, J. & Ball, J. 2012 A new method of calculating electrical conductivity with applications to natural waters. *Geochimica et Cosmochimica Acta* **77**, 369–382.

Merzouk, B., Gourich, B., Sekki, A., Madani, K., Vial, C. & Barkaoui, M. 2009 Studies on the decolorization of textile dye wastewater by continuous electrocoagulation process. *Chemical Engineering Journal* **149** (1–3), 207–214.

Moore, D. S. 2007 *The Basic Practice of Statistics*. WH Freeman, New York.

Moreno, H., Parga, J. R., Gomes, A. J. & Rodríguez, M. 2013 Electrocoagulation treatment of municipal wastewater in Torreon Mexico. *Desalination and Water Treatment* **51** (13–15), 2710–2717.

Perry, R., Green, D. & Maloney, J. 1984 *Perry's Chemical Engineers' Handbook*. McGraw-Hill, New York.

Phalakornkule, C., Mangmeemak, J., Intrachod, K. & Nuntakumjorn, B. 2010 Pretreatment of palm oil mill effluent by electrocoagulation and coagulation. *Science Asia* **36** (2), 142–149.

Pokhrel, D. & Viraraghavan, T. 2004 Treatment of pulp and paper mill wastewater – a review. *Science of the Total Environment* **333** (1), 37–58.

Raj, A., Reddy, M. & Chandra, R. 2007 Decolourisation and treatment of pulp and paper mill effluent by lignin-degrading *Bacillus* sp. *Journal of Chemical Technology and Biotechnology* **82** (4), 399–406.

Rajeshwari, K. V., Balakrishnan, M., Kansal, A., Lata, K. & Kishore, V. V. N. 2000 State-of-the-art of anaerobic digestion technology for industrial wastewater treatment. *Renewable Sustainable Energy Reviews* **4** (2), 135–156.

Shankar, R., Singh, L., Mondal, P. & Chand, S. 2014 Removal of COD, TOC, and color from pulp and paper industry wastewater through electrocoagulation. *Desalination and Water Treatment* **52** (40–42), 7711–7722.

Shawwa, A., Smith, D. & Sego, D. 2001 Color and chlorinated organics removal from pulp mills wastewater using activated petroleum coke. *Water Research* **35** (3), 745–749.

Solak, M., Kılıç, M., Yazıcı, H. & Şencan, A. 2009 Removal of suspended solids and turbidity from marble processing wastewaters by electrocoagulation: comparison of electrode materials and electrode connection systems. *Journal of Hazardous Materials* **172**, 345–352.

Sridhar, R., Sivakumar, V., Prince Immanuel, V. & Prakash Maran, J. 2011 Treatment of pulp and paper industry bleaching effluent by electrocoagulant process. *Journal of Hazardous Materials* **186** (2–3), 1495–1502.

Terrazas, E., Vázquez, A., Briones, R., Lázaro, I. & Rodríguez, I. 2010 EC treatment for reuse of tissue paper wastewater: aspects that affect energy consumption. *Journal of Hazardous Materials* **181** (1–3), 809–816.

Varank, G., Guvenc, S. Y., Gurbuz, G. & Engin, G. O. 2016 Statistical optimization of process parameters for tannery wastewater treatment by electrocoagulation and electro-Fenton techniques. *Desalination and Water Treatment* **57** (53), 25460–25473.

Vasudevan, S., Lakshmi, J. & Sozhan, G., 2012 Studies on the removal of arsenate from water through electrocoagulation using direct and alternating current. *Desalination and Water Treatment* **48** (1–3), 163–173.

Verenich, S., Laari, A. & Kallas, J. 2000 Wet oxidation of concentrated wastewaters of paper mills for water cycle closing. *Waste Management* **20** (4), 287–293.

Wang, Q. G., Lee, T. H., Fung, H. W., Bi, Q. & Zhang, Y. 1999 PID tuning for improved performance. *IEEE Transactions on Control Systems Technology* **7** (4), 457–465.

Xu, Y., Jiang, J. Q., Quill, K., Simon, J. & Shettle, K. 2009 Electrocoagulation: a new approach for the removal of boron containing wastes. *Desalination and Water Treatment* **2** (1–3), 133–140.

Yadav, A. K., Singh, L., Mohanty, A., Satya, S. & Sreekrishnan, T. R. 2012 Removal of various pollutants from wastewater by electrocoagulation using iron and aluminium electrode. *Desalination and Water Treatment* **46** (1–3), 352–358.

Zaied, M. & Bellakhal, N. 2009 Electrocoagulation treatment of black liquor from paper industry. *Journal of Hazardous Materials* **163** (2–3), 995–1000.

Ziegler, J. G. & Nichols, N. B. 1942 Optimum settings for automatic controllers. *Transactions of ASME* **64** (11), 759–765.

First received 21 April 2017; accepted in revised form 12 September 2017. Available online 26 September 2017

Downloaded from http://iwaponline.com/wst/article-pdf/76/12/3410/241768/wst076123410.pdf
by guest